Estimating the Energy Dependence of the Electron-Hadron Discrimination in STAR using the Electromagnetic Calorimeter

S. Chattopadhyay, T.M. Cormier, A. I. Pavlinov, V. L. Rykov and A. V. Stolpovsky
Wayne State University

and

K. E. Shestermanov and A.N. Vasiliev
IHEP Protvino

ABSTRACT

Electron-hadron discrimination is studied with experimental data obtained in a 1998 test beam run and in simulations of the Electromagnetic Calorimeter (EMC) including the pre-shower detector (PSD) and shower-maximum detector (SMD) elements.   The emphasis of the study is to provide better estimates of the ability of this combination of detectors to provide electron identification in the low energy region (0.5 GeV to 5.0 GeV) which will be important in the study of J/ψ and perhaps ϕ -> e^+e^- at low P_T.

I.   Introduction

STAR, with its very large acceptance and event-by–event capability will be an important tool in the study of vector meson production and suppression in heavy ion collisions at RHIC, provided adequate electron identification and hadron suppression can be achieved. In both cases of immediate interest, ϕ -> e^+e^- and J/ψ , electron spectra must be observed against an overwhelmingly more intense hadron background. The efficiency of electron identification and the corresponding hadron rejection factor thus virtually determine the phase space, if any, for these particles in STAR   Difficult as these measurements will be, however, they provide direct insight into matters central to the physics of the quark-gluon plasma. A study of the suppression of J/ψ and its P_T dependence in particular, is thought to provide one of the few direct handles on deconfinement and color screening while the branching ratio of ϕ -> ee to ϕ -> KK may be a direct observable for chiral symmetry restoration in the hot dense matter produced in AuAu collisions.

In the present study, we focus on relatively low energy electrons using the EMC because this is the most difficult and least well understood region for electron identification and because it is the region most relevant to the heavy ion program.   Other detector elements in STAR beyond the scope of the present study, in particular the Time of Flight (TOF) and RICH detectors as well as TPC dE/dx can also contribute significantly to electron identification.   Unfortunately, both TOF and RICH have acceptances that will be too

small, at least initially, to contribute significantly to vector meson studies although they will provide important extensions to STAR's particle identification capabilities for more abundant particles. TPC dE/dx, on the other hand, will make some contribution to electron identification both in the relativistic rise region and below about 300 to 400 MeV where pions begin to have β significantly different from one (>5% at 400 MeV). This additional capability, which comes with STAR's full acceptance can be combined with the EMC's hadron suppression studied here. In vector meson studies each additional contribution to the hadron suppression enters twice in the e^+e^- invariant mass spectrum.

In the present study, we use experimental test beam data and GSTAR simulations to examine the response of the calorimeter to single electrons or pions at several momenta from 0.5 to 5.0GeV/c. This energy region is chosen to provide new information on the combined calorimeter system's performance in a region where the pre-shower detector is expected to contribute significantly to electron identification. Furthermore, this energy region allows some validation of our simulations with experimental test beam data which exist up to 5.0 GeV/c. In particular, we use the 1998 test beam data taken with a close to final version of the calorimeter. These simulations and test beam data explore the response of the calorimeter alone to ideal events with single particles of known momenta. In real STAR events, cluster finding and contamination, track matching and cluster splitting across calorimeter cracks will degrade the calorimeter's performance compared to the results reported here. On the other hand, the study hadron suppression factors greater than 100, as encountered in the present work, requires more statistics than is easily achievable at present with a full analysis of full AuAu events. We thus regard the present results as a good first estimate of the energy dependence of the calorimeter as an electron identifier in STAR with the caveat that, at the very least, overall electron detection efficiency will suffer somewhat in real events from the calorimeter occupancy. More detailed simulation and experimental studies will follow including additional test beam results.

Previous simulation studies of electron-hadron discrimination in STAR have been reported. An early study by Derevschikov et al., in STAR Note 305 also includes an analysis of $\pi_o - \gamma$ separation using an early SMD design. More recently, LeCompte, in STAR Note 306 studied the possible inclusion of the pre-shower detector in an early conceptual version.

In the following section we will discuss the calorimeter "as-built" configuration and, in qualitative terms, those signals which are sensitive to electron-hadron (e-h) discrimination. This is followed in section III by a discussion of the GSTAR simulations of these seven signals along with a neural network analysis of the resultant e-h discrimination they afford. In this section we also study the dependence of our predicted e-h discrimination on the choice of a specific hadronic cascade model. Finally, in section IV we provide an analysis, taking proper account of correlations, of the individual contributions to e-h discrimination provided separately by the tower energy measurements, the shower maximum detector and the pre-shower detector. We then examine the 1998 test beam results of e-h discrimination based on tower energy measurements which combined with our simulations of the (correlation corrected) e-h discrimination provided by the pre-shower detector and the shower maximum detector to

form a hybrid "best current estimate" of the energy dependence of the overall e-h discrimination.

II. The Detector elements and signals sensitive to electron-hadron discrimination

Figure 1 shows the layered geometry of the STAR's sampling electromagnetic calorimeter (EMC). Twenty one layers of scintillator alternate with twenty layers of Pb each 5mm (approximately $1X_o$) thick. Layers 1 and 2 of scintillator are each 6mm thick and are summed optically and read out as the pre-shower signal. Scintillator layers 3 through 21 are each 5mm thick and are summed together optically along with layers 1 and 2 to constitute the full energy signal. The 6 mm thickness for layers 1 and 2 is chosen together with the optical coupling scheme such that these layers contribute the same number of photo-electrons per unit energy deposition to the energy sum as the other 19 layers. The shower maximum detector (SMD), located after the fifth layer of Pb, is a double layer wire chamber with independent strip readout for the η and ϕ directions which permit shower intensity, position and shape measurements. The reader is referred to STAR Note 351 for further details of the EMC and SMD performance.

In our simulation study of EMC hadron suppression capability, we include for the first time the "as built" geometry of the pre-shower detector (PSD). This detector component, as we will show, is important for low energy hadron suppression. Previous experimental studies of the calorimeter's electron-hadron discrimination have been reported. Bennett et al., STAR Note 351, based on 1997 test beam results, conducted one of the first detailed experimental studies of the performance of the EMC as a function of energy. Their work included the EMC tower response in detail and a limited study of the shower maximum detector at the single electron energy of 5.0 GeV. The pre-shower detector was not included in the EMC design at the time of their work.

259.92mm

193.04mm

r=2629.99mm

69.85mm

linear bearing track

33.44mm

91.99mm

linear bearing carriage

24.99mm

back plate-carriage interface plate

back plate

compression plate key

compression plate

Belleville washers

Sc 21

Sc 20

Sc 19

Sc 18

Sc 17

strap

Sc 16

Sc 15

Lead plate

Sc 13

Sc 12

Scintillator tile

Sc 11

Sc 10

Sc 9

Sc 8

Sc 7

302.99mm

SMD

Sc 5

Sc 4

Pre
Shower
Detector

Sc 3

Sc 2

front plate

r=2235

228.16mm

Figure 1.

In the present set of simulations, we consider all of the information potentially available from the EMC towers, the SMD and the PSD. The following seven parameters are considered: E/p, E_{SMD}, $\Delta\eta$, $\Delta\phi$, σ_η, σ_ϕ, and E_{PSD}.

1. E/p: The EMC tower energy provides a high resolution, linear measure of the full energy of electrons strike it. Hadrons, on the average, even those which shower within the calorimeter, typically deposit far less than their total energy in a tower. A comparison of tower energy to tracked momentum, E/p, thus is an electron identifier who's effectiveness varies with the momentum resolution of the TPC and the calorimeter's energy resolution. The latter scales as ~ 15%/ $\sqrt{E}$ and thus E/p selection improves with increasing energy until dominated by the TPC resolution at high P_T.

2. E_{SMD}, Shower Maximum Detector energy deposition: The SMD is located within the calorimeter at a depth of approximately 5.6 radiation lengths. This number includes

the calorimeter itself plus other material directly in front of the calorimeter. At this depth, The SMD is near the maximum density of electromagnetic showers with energies greater than about 1 - 2 GeV whereas hadronic showers have maximum density of energy deposition near one interaction length (e.g. 17 cm for Pb) and exhibit a much broader longitudinal distribution. This distinction renders the energy deposition in the shower maximum detector useful for hadron suppression. The electromagnetic shower maximum depth varies logarithmically with energy and consequently this signal is useful over a very wide energy range $> 1\text{-}2$ GeV. At lower energies, < 1 GeV, the shower depth quickly becomes less than $5.6X_o$ and the SMD contributes little to electron discrimination. Hadrons which pass a SMD cut tend to be those for which hadronic showers occur early in the detector and particularly those which produce leading π_o's. Consequently, hadrons which pass an SMD cut tend to be those depositing larger than average fraction of their total energy in the calorimeter and are therefore those that are most difficult to remove with the E/p cut. This is an example of the kind of correlations that render combined detectors less effective than the simple product of their individual hadron rejection powers.

The potential to use the energy deposition signals from the two SMD layers $E_{SMD(\eta)}$ and $E_{SMD(\phi)}$, independently, has not been explored in the present work. While these signals are strongly correlated on the average, their fluctuations are less so and preliminary experimental studies have shown that there may be a significant advantage to expanding the above parameter list from seven to eight. This will be explored in the future.

3. $\Delta\eta$, $\Delta\phi$, Shower Position: For charged particles, TPC tracking determines the expected hit position at the calorimeter with mm-like precision. The response of the shower maximum detector is used to reconstruct the hit position in the η and ϕ directions from the centroids of the measured transverse shower distributions. Hadronic showers, which are typically incompletely developed by the $5.6\ X_o$ depth of the SMD, show centroids of energy deposition which can fluctuate substantially with respect to the extrapolated track position from the TPC. Thus the measured errors in the reconstructed versus extrapolated hit positions, $\Delta\eta$, $\Delta\phi$, can be used to provide additional hadron suppression in the energy range where good SMD signals are observed, typically > 1 GeV.

4. σ_η, σ_ϕ, Shower Shape: Electromagnetic showers exhibit compact shapes with $\sim 95\%$ of the shower energy contained in a cylinder of radius equal to twice the Moliere radius (e.g., $2R_M = 3.2$ cm for Pb). On the other hand, the transverses dimensions of hadronic showers are much larger, approximately one interaction length, λ, when fully developed (at depth $\sim\lambda$). At the SMD depth, incompletely developed hadronic shower transverse dimensions exhibit substantial fluctuations, but may still be significantly larger than corresponding electromagnetic showers. Thus the standard deviations of the observed shower distributions in the η and ϕ directions, σ_η, σ_ϕ, reconstructed from the measured shower profiles in the SMD, are expected to contribute to hadron suppression, again, for electron energies approximately > 1 GeV.

5. E_{PSD}, Pre-Shower Detector energy deposition: The first and second scintillating layers of the calorimeter comprise the pre-shower detector.   A typical electron exhibits a substantially higher dE/dx than hadrons even before the initiation of an electromagnetic shower and ~63% of electrons will shower before scintillator layer 1 and ~84% before layer 2. This is to be compared with the interaction probability for hadrons (considering only the Pb) of approximately 3% before the first layer and 6% before the second layer. Thus, energy distributions for electrons and hadrons differ substantially in the pre shower detector in a manner which will be almost independent of energy.   Consequently, the pre-shower detector is particularly important to the overall hadron suppression for energies less than about 1.5 GeV.

III. GSTAR Simulations of the Calorimeter Performance

Each of the seven signals described above is correlated to a lesser or greater degree with the other 6 and, furthermore, the extent of the correlation between any two signals may vary with energy.   To correctly account for these correlations in an analysis of electron-hadron discrimination, a simultaneous analysis of all 7 signals is required. Furthermore, to ascertain the contribution of any one signal to the overall hadron suppression, one must compare the hadron suppression achieved with all seven signals to that achieved when the detector in question is removed from the analysis. In this way one can calculate the correlation corrected contribution of any single or any group of signals. To enable this type of calculations, we have chosen to apply a neural network analysis of GSTAR simulated data in which a seven node network is trained to distinguish electrons and hadrons. Our data sets consisted of samples of pure π^+ or e^+ at momenta of 0.5, 1.0, 2.0 and 5.0/c GeV. Electron statistics were typically 5000 and hadron statistics were typically 15000.   GSTAR calculations were performed for the pair of $\eta=0$ tower ($\eta=0.0$ to 0.05 in STAR) which reside within a single module with particles incident upon an area which allows us to avoid the complication of correcting for energy sharing across the ϕ crack between neighboring modules.

For both the tower energy and pre shower energy depositions, ADC channels were computed using measured photo electron yields of 3 photo electrons per MeV of energy deposition and were smeared with a realistic simulation of the photomultiplier single photoelectron response. This latter effect is particularly important for the pre shower detector where the mean signal for a minimum ionizing particle produces just 5.5 photo electrons from the two layers of the pre shower detector combined. At present, in the absence of a good model for the full system response of the shower maximum detector, we work directly with GEANT energy depositions.   Electronic noise is expected to degrade the performance of the shower maximum detector only at the very lowest energies where, in any event, the pre shower detector is more important. The momentum of the incident particle is smeared by an amount consistent with the expected performance of the STAR TPC, before using it in relation to the measured calorimeter energy to produce a "measured" E/p parameter.

Figure 2. Output of the seven node neural network as trained for 1 GeV/c electrons and 1 GeV/c hadrons.
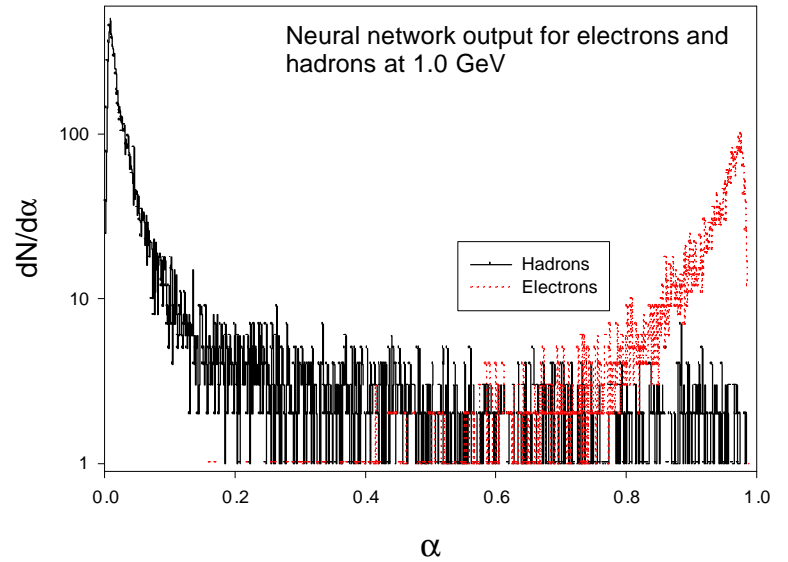
Figure 2 shows the output of the seven node neural network for 1.0 GeV/c electrons and hadrons. The network has been trained such that hadrons produce the maximum near $\alpha=0$ and electrons near $\alpha=1$.   Given this plot at each energy, the effectiveness of electron-hadron discrimination can be characterized by the hadron efficiency ε_h and the electron efficiency ε_e obtained by integrating data such as in figure 2 over the appropriate interval of α from some α_{cut} to $\alpha=1$.   As α_{cut} is varied, the functional dependence of ε_h on ε_e is determined. The hadron suppression factor, $h =1/\varepsilon_h$ computed in this manner at each corresponding electron efficiency is shown as the solid points in figures 3, 4 and 5 for 0.5, 1.0 and 5.0 GeV/c respectively. The open points show the product $h\varepsilon_e$.   Roughly speaking, the signal to background ratio for a single electron measurement is $(M_e/M_h)(\varepsilon_e/\varepsilon_h)$ where M_e and M_h are the electron and hadron multiplicities. Thus the product $h\varepsilon_e$ is the signal to background ratio in the case of equal numbers of hadrons and electrons.

Figure 3. Predicted hadron suppression at 0.5 GeV/c based on all three components of the EMC
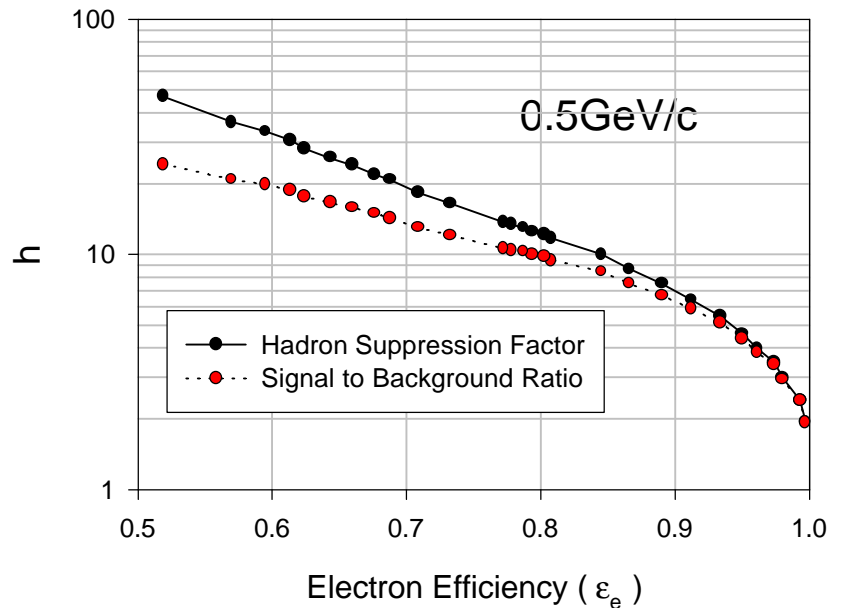
Figure 4. Predicted hadron suppression at 1.0 GeV/c based on all three components of the EMC
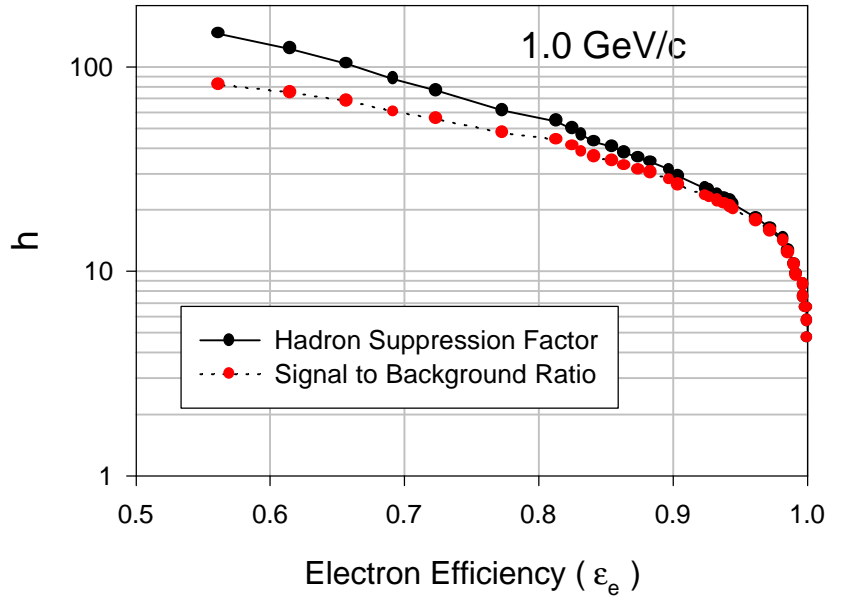
The present results which include a more complete analysis of the SMD and also include the PSD, give hadron suppression factors which range from 7 to 115 at 90% efficiency and between 50 and over 900 at 50% efficiency for electron momenta between 0.5 and 5 GeV/c. The corresponding hadron suppression factors from STAR Note 305 at 5 GeV/c and 90% efficiency, for example, is over a factor of 6 worse with most of this difference coming from our full analysis of the SMD, the inclusion of the PSD and allowing asymmetric(relative to the mean value) E/p cuts through the neural network analysis.

Figure 5. Predicted hadron suppression at 5.0 GeV/c based on all three components of the EMC
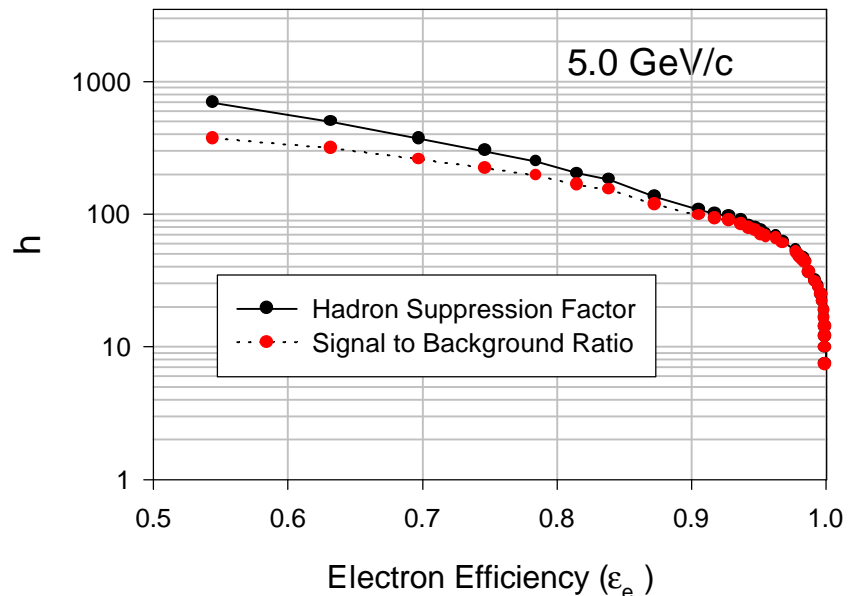
We have studied the sensitivity of our calculations to the hadronic shower simulation model used within GEANT. Results have been obtained for both of the standard hadronic models, GHEISHA and FLUKA. The results shown to this point and those of STAR Note 305 were all obtained with the GHEISHA simulation of hadronic showers. Apriori, we expect considerable sensitivity in e-h discrimination to the details of the calculated hadronic cascade. This follows from the fact that the E/p cut dominates hadron suppression at all but the lowest energies and this cut is very sensitive to the details of the hadronic energy deposition in the calorimeter. The shallow depth of the calorimeter in terms of hadronic interaction lengths which results in E/p being a powerful discriminator in the first place, also leads to large fluctuations in hadronic energy deposition. Modeling these fluctuations correctly, particularly in the tail of the distribution, where the electron peak sits, is essential to a good prediction of the hadron suppression resulting from E/p. At 5.0 GeV/c with 90% electron efficiency, for example, GHEISHA gives only ≈2.5% of the hadrons passing the electron E/p cut. Figure 6, which shows the simulated electron and hadron spectra at 5 GeV/c underscores the problem. Knowledge of the high energy tail of the hadron energy deposition distribution at a demanding level of precision is clearly required since, as is apparent from figure 6, even a very minor redistribution of a few percent of the total hadrons could result in a factor of two or more change in the predicted number of hadrons passing the electron cut.
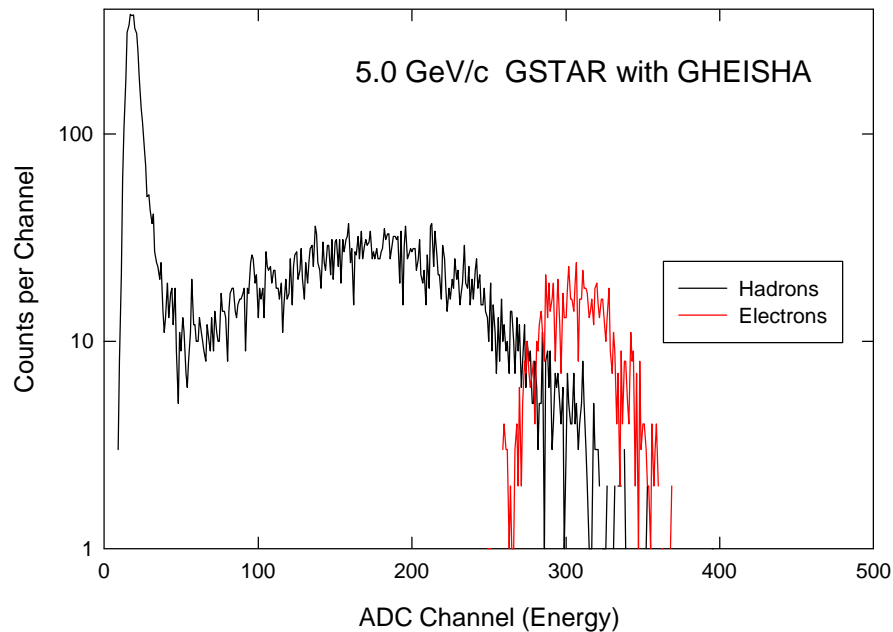
Figure 6. Simulated hadron and electron energy deposition spectra obtained in GSTAR with the GHEISHA hadronic cascade model.

To quantitatively test this model sensitivity, we also ran all of our simulations with the hadronic cascade package FLUKA. We find that FLUKA gives consistently larger hadronic energy deposition in our geometry resulting in a larger fraction of hadrons passing electron cuts. Table 1 compares predicted hadron suppression factors for the two models at 90% electron efficiency.

Table 1. Comparison of relative hadron suppression factors computed with GHEISHA and FLUKA at 90% electron efficiency.

$p_{electron}$ (GeV/c)	h(GHEISHA)/h(FLUKA)
0.5	2.55
5.0	2.13

This model dependence results almost entirely from differences in hadronic energy deposition with negligible difference appearing in the PSD or SMD simulations. This is easy to understand. All but a few percent of hadrons deposit energy in the PSD by ionization energy loss, dE/dx. Consequently, the PSD contribution to h is largely insensitive to the details of the early shower development of those hadrons which do shower. For the SMD, we find that its dominant contribution to h relies on the fact that electromagnetic showers are compact in transverse dimension and well located at the extrapolated track position. Furthermore, as in the PSD, most of the hadron suppression provided by the amplitude of the SMD signal is for hadrons which have not interacted in the first $5X_o$ of the detector which therefore depends only on the total cross section and not the details of the subsequent hadronic cascade. Consequently, we expect the PSD and SMD simulations to be more robust with respect to the choice of any particular hadronic cascade model.

Figure 7. Energy deposition spectra In the pre shower detector compared for FLUKA and GHEISHA calculations at 5 GeV/c. The corresponding electron result is shown to illustrate the electron-hadron discrimination.
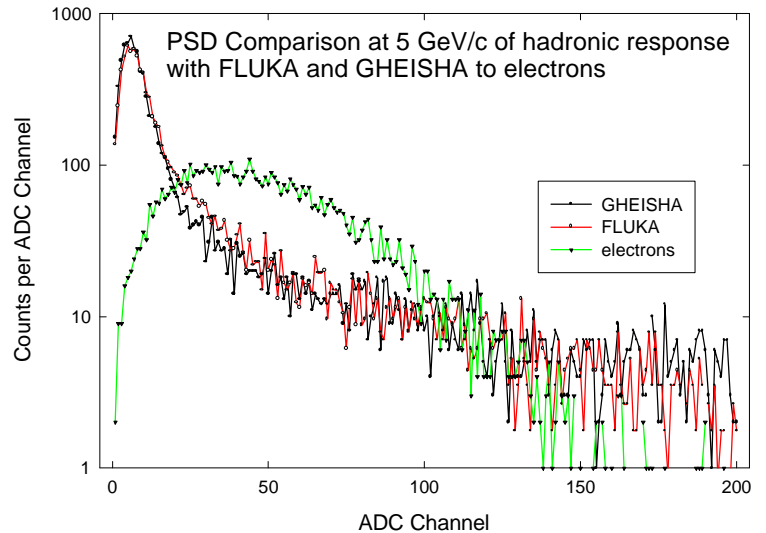
These expectations are verified in figures 7 and 8 where SMD and PSD energy deposition spectra are presented for FLUKA and GHEISHA calculations and compared with the corresponding energy deposition for electrons. The model dependence seen in these figures is at the few percent level or less.

Figure8. Energy deposition spectra in the shower maximum detector Compared for FLUKA and GHEISHA calculations at 5 GeV/c. The corresponding electron result is shown to illustrate the electron-hadron discrimination.
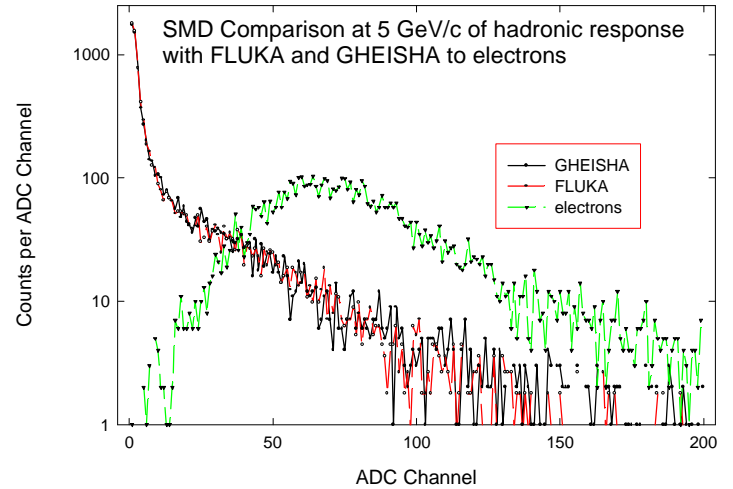
IV. Results of the 1998 test beam and a hybrid estimate of e - h discrimination based on simulations and experiment.

The 1998 test beam at the AGS afforded an opportunity to take a first look at the e - h discrimination of the final version of the EMC detector systems under more nearly realistic experimental conditions. In the present STAR Note we will look only at the e - h discrimination provided by the EMC tower energy measurements. We limit the presentation to the tower energies at this point because the SMD electronics used to readout the SMD during the 1998 tests were of a very preliminary design which allowed only a small data set to be accumulated and were known to be inferior in terms of noise performance compared to subsequent prototype generations. For the SMD, we have better test beam results from the 1997 test. As far as the PSD is concerned in the 1998 tests, mechanical failures of their prototype fiber design resulted in an incomplete data set so these measurements must be repeated.

The experimental hadron suppression factors for an $\eta=0$ tower are shown in figure 9 with the corresponding signal to background ratios, again defined as $h\varepsilon_e$ presented in figure 10.

*Figure 9.
Experimental hadron
suppression factors as
measured in the 1998
test beam using only
tower energy
measurements and the
known momentum of
the beam, E/p.*

1998 STAR EMC test beam data
Hadron suppression factors from E/p
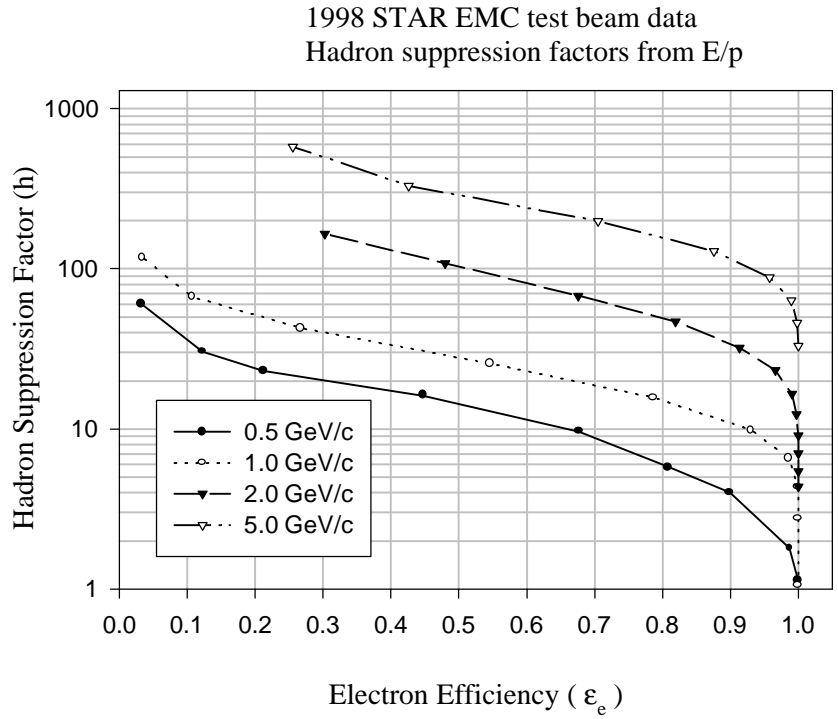
*Figure 10. Experimental
 h**e**$_e$ for an **h**=0 tower
deduced from the
measurements shown in
figure 9.*

Signal to Background Ratio (hε_e)
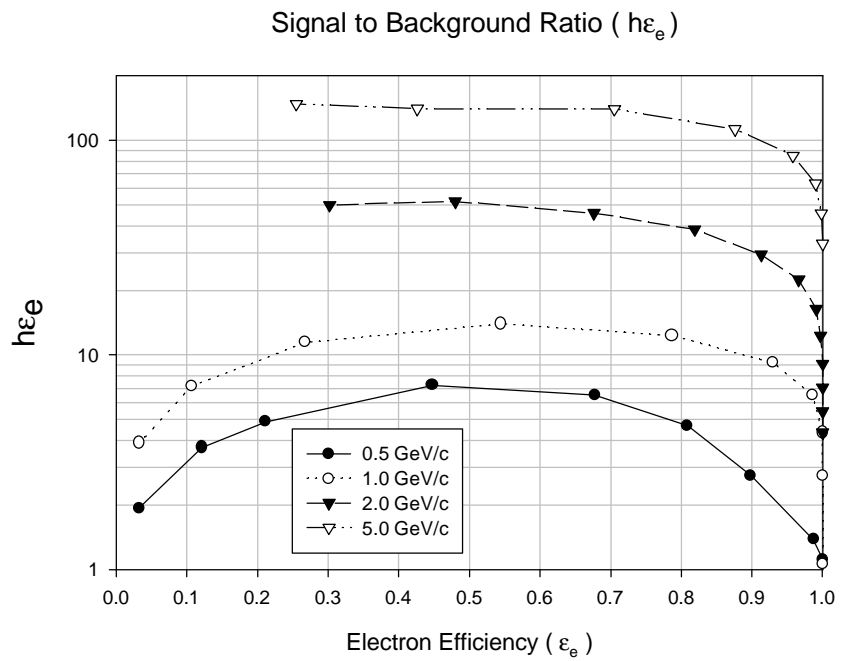
The above experimental data can be used to check the reliability of the estimate of
electron hadron discrimination provided by the simulations of the preceding sections. In

particular, since the majority of the model dependence comes from the tower energy E/p comparison, we can use the experimental data on this parameter to considerably reduce the model dependent uncertainty in h versus ε_e. As discussed above, the simulations of the PSD and SMD are relatively more robust with respect to the details of the hadronic cascade model. Consequently, a hybrid estimate of the total hadron suppression which takes the E/p contribution from experiment is likely to be more reliable. This is explored below.

First, it is interesting to compare our simulated h based on E/p only with the corresponding measurement from the 1998 test beam. This comparison is shown in figure 11. The simulated hadron suppression based on E/p only, call it h(E/p), is shown for the GHEISHA calculations compared with h deduced from the 1998 test beam data again for E/p only. The calculations do a remarkable job of reproducing h at 0.5 and 1 GeV/c, perhaps underestimating h at lower electron efficiency by something on the order of 15 to 20%. At 5 GeV/c, however, the model considerably underestimates h by over a factor of two to three. This situation is traceable to the predicted evolution with energy of the high energy tail in the hadronic energy deposition spectrum. GHEISHA, and even more so FLUKA, predict a larger fraction of nearly full energy deposition events for hadrons in this energy range which accounts for the lower simulated h. It bears repeating that although the error in h is substantial, it results from a very small error in the calculated hadronic energy distribution.

Figure 11. Experimental hadron suppression factors obtained in the 1998 test beam using tower E/p compared to the results of our simulations using the GHEISHA hadronic cascade model.

Hadron suppression based on E/p only using GHEISHA
Compared to the 1998 test beam results
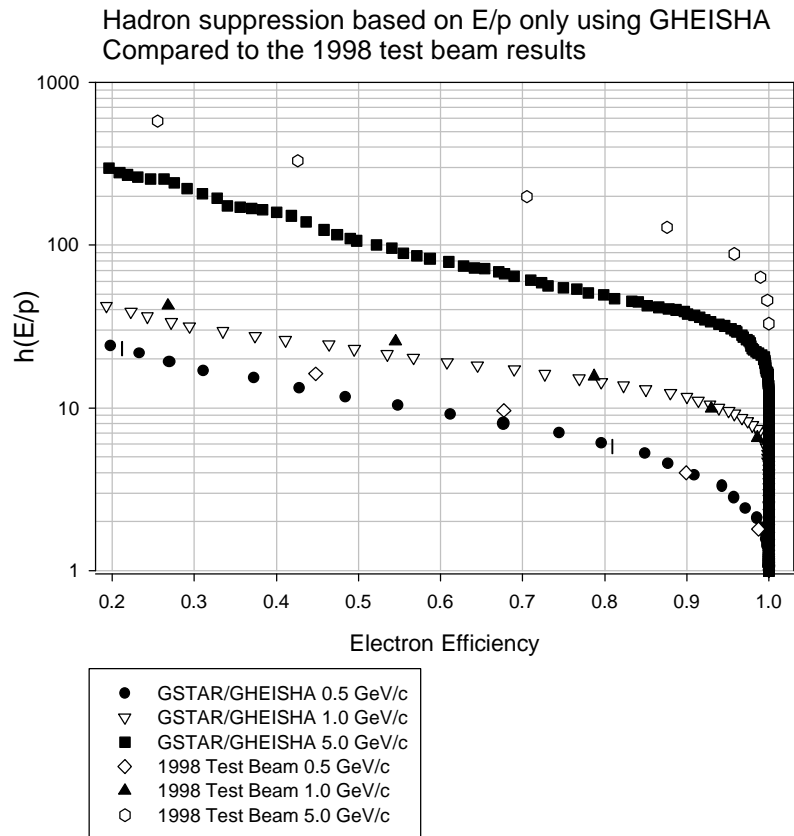
The experimental test beam data can be used to obtain a "best current estimate" of e - h discrimination. To do this we apply the simulated value of the combined hadron suppression provided by the SMD and the PSD (when used in conjunction with tower energy measurements, i.e. correlation corrected) to the experimental hadron suppression from E/p observed in the test beam. The combined hadron suppression from the PSD and the SMD in the presence of the E/p cut can be extracted from our simulations by comparing the hadron suppression obtained in the neural net analysis of all seven EMC parameters with the hadron suppression obtained from a single one dimensional cut on tower energy deposition (E/p) as shown in figure 11.   When included in a full analysis using all seven parameters, the correlations of the three detector components (EMC towers, SMD, PSD) are properly accounted for. This procedure therefore results in correlation corrected suppression factors for the combined PSD and SMD, call it h(SMD,PSD), that are substantially smaller than obtained if either or both of these detector elements are analyzed separately. Stated equivalently, h(SMD,PSD) is defined such that the overall hadron suppression is correctly given by the relation

$$h = h(SMD,PSD)h(E/p) \qquad\qquad 1.$$

where h(E/p) is as shown in figure 11.   We find that this correlation corrected contribution to h from the PSD and SMD is a smooth function of electron efficiency and energy which rises a factor of 2.75±.25 as the electron efficiency varies from 90% to 50%, nearly independent of energy and which rises a factor of $2.2 \pm .15$ as a function of energy from 0.5 GeV to 5.0 GeV, independent of efficiency.   The errors noted here characterize the maximum observed deviation of these factors.

Figure 12. The contribution to hadron suppression produced by the shower maximum detector and the pre shower detector as reduced by correlations with the tower energy deposition.

Simulated hadron suppression provided by the SMD and the PSD alone.
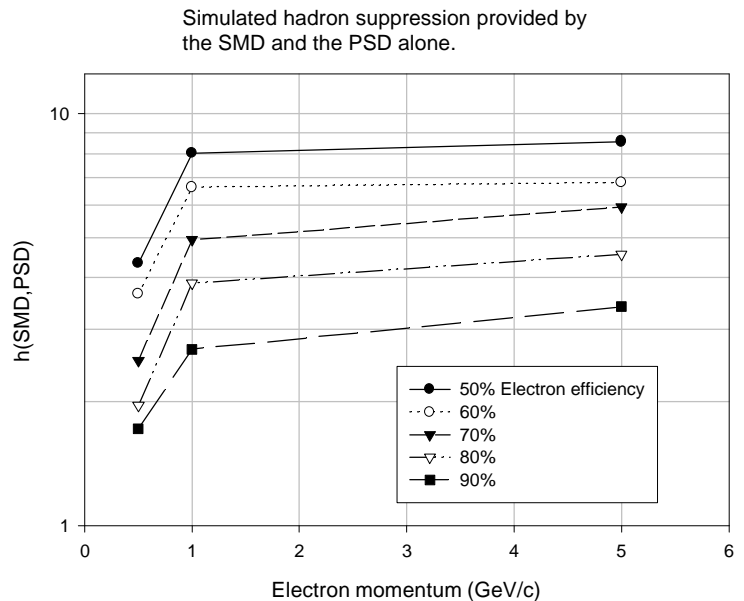
The combined SMD-PSD hadron suppression factors, h(SMD,PSD) are shown in figure 12 as a function of electron momentum for several electron efficiencies. Figures 13 and 14 show this same data arbitrarily scaled to illustrate the simple, scaling-like dependence that h(SMD,PSD) exhibits on electron energy and efficiency.
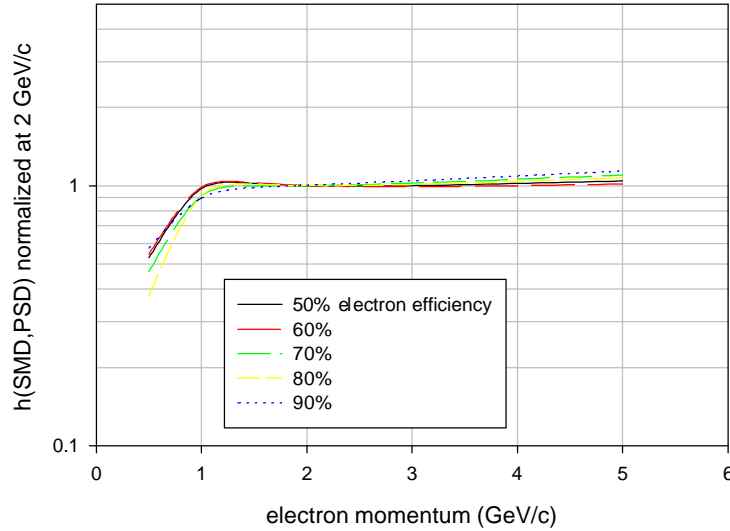
Figure 13. The combined, correlation corrected, hadron suppression due to the shower maximum detector and pre shower detector versus electron momentum, normalized at 2 GeV/c to show the near universal dependence on electron momentum in this energy range.

Figure 14. The combined, correlation corrected, hadron suppression due to the shower maximum detector and pre shower detector versus electron momentum, normalized at70% electron efficiency so as to show the near universal dependence on electron efficiency in this energy range.

Scaled h(SMD,PSD) versus electron efficiency
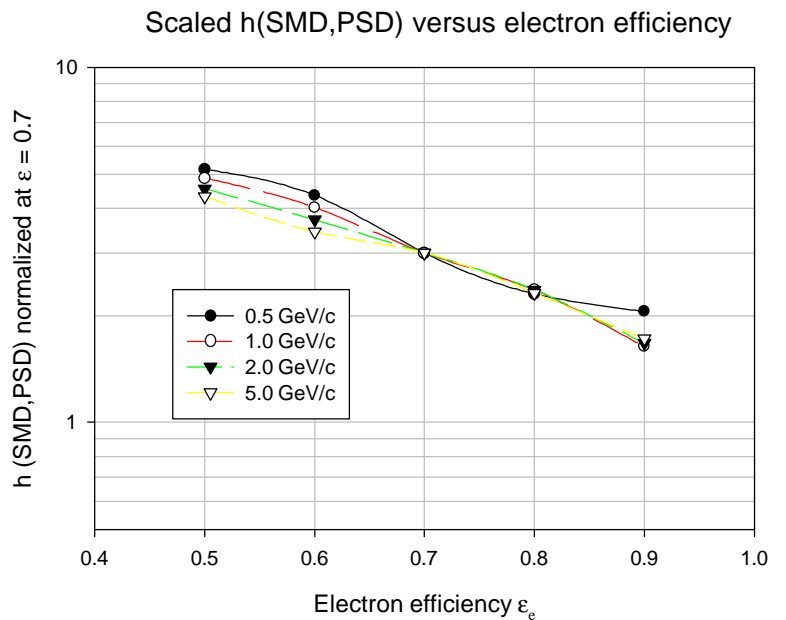
The simple dependence that h(SMD, PSD) exhibits on ε_e allows us to estimate this quantity at 2 GeV/c as shown on figure 14. These factors, h(SMD, PSD) given in table 2, can now be used in conjunction with the hadron suppression observed in the 1998 test beam for E/p only, h(E/P), (figure 11) to obtain our current best estimate of the overall performance of the STAR EMC as an electron detector shown in figure 15.

Table 2. Hadron suppression factors as a function of energy and electron detection efficiency for the SMD and PSD as reduced by the correlation with the EMC towers, h(SMD, PSD).

	Electron Efficiency				
E(GeV)	50%	60%	70%	80%	90%
0.50	4.33	3.65	2.52	1.60	1.72
1.00	8.01	6.63	4.94	3.88	2.68
2.00	8.20	6.70	5.40	4.25	3.00
5.00	8.56	6.81	5.94	4.56	3.40

It is interesting to note that the sudden drop in hadron suppression by the SMD/PSD combination which occurs below 1.0 GeV is a result of the onset of near full absorption of these low energy electromagnetic showers before reaching the SMD.

V. Conclusions

Our final result is shown in figure 15. This is our current best estimate of the achievable hadron suppression in electron measurements with the STAR EMC. Relying as we do on both simulations for h(SMD, PSD) and experimental data h(E/p), we have attempted to minimize the model dependence in these results.

It bears emphasis that these results are a property of the calorimeter and expected to apply in an ideal environment which is probably well approximated in low multiplicity events in STAR. In high multiplicity events, one has the additional complications of cluster reconstruction in the face of contaminating tracks, neutral backgrounds etc. The combined effect of these complications will be to reduce the electron reconstruction efficiencies compared to those which appear in figure 15. This problem is currently under study although we may already anticipate from preliminary work that electron reconstruction efficiencies will not be significantly degraded above 1 to 1.5 GeV but are likely to be reduced below 1 GeV where some type of isolation cut might need to be imposed to achieve hadron suppression similar to that in figure 15.

Our results show that hadron suppression varies by approximately a factor of 70 at constant electron efficiency while at constant hadron suppression, say h=100, the electron efficiency varies only slightly more than a factor of 2. This fact can be used to advantage

in real applications of the calorimeter where electrons associated with the desired process will be typically far more abundant at lower P_T than at high P_T. In this situation, lower electron efficiencies can be tolerated exactly where they are needed to achieve higher hadron suppression.
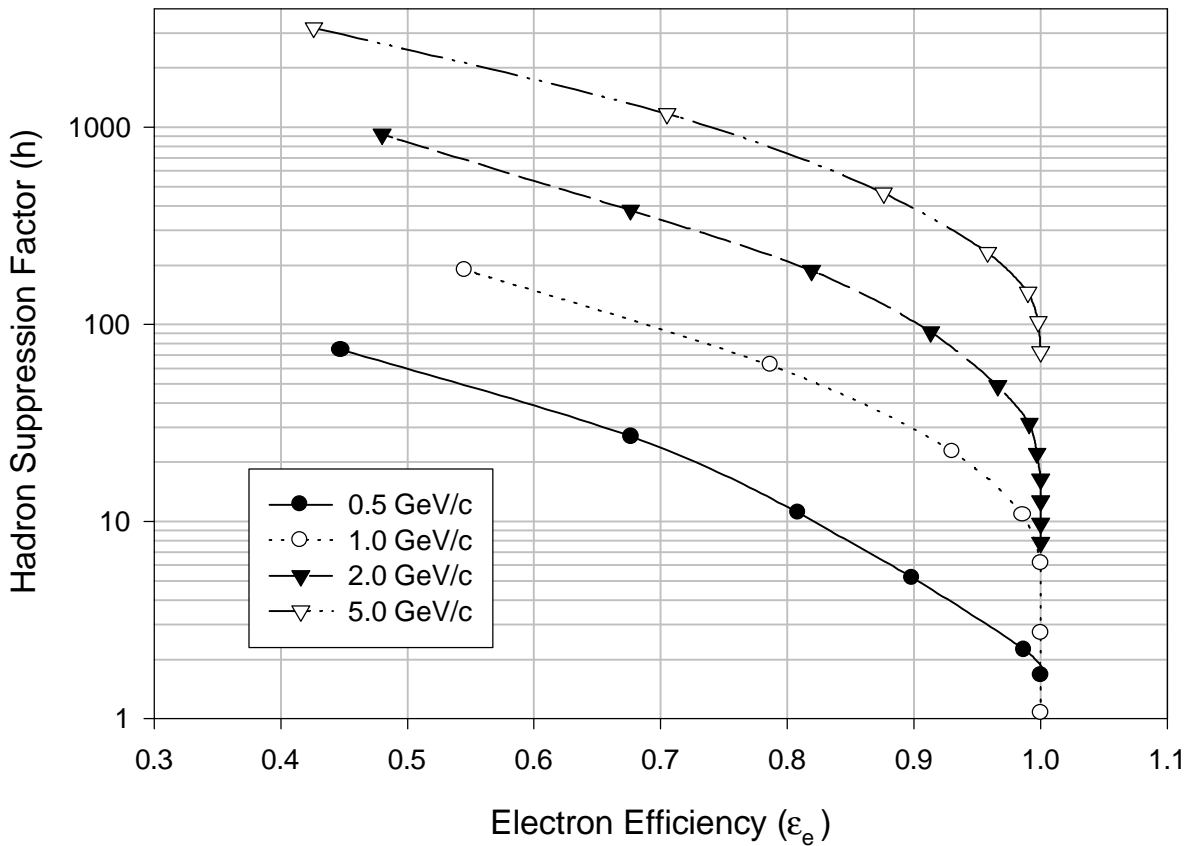
Figure 15. Final, best current estimate, hadron suppression factors based on experimental results for the dominant hadron suppression which follows from E/p combined with what we have argued are robust simulations of the correlation corrected hadron suppression provided by the shower maximum detector and the pre shower detector.